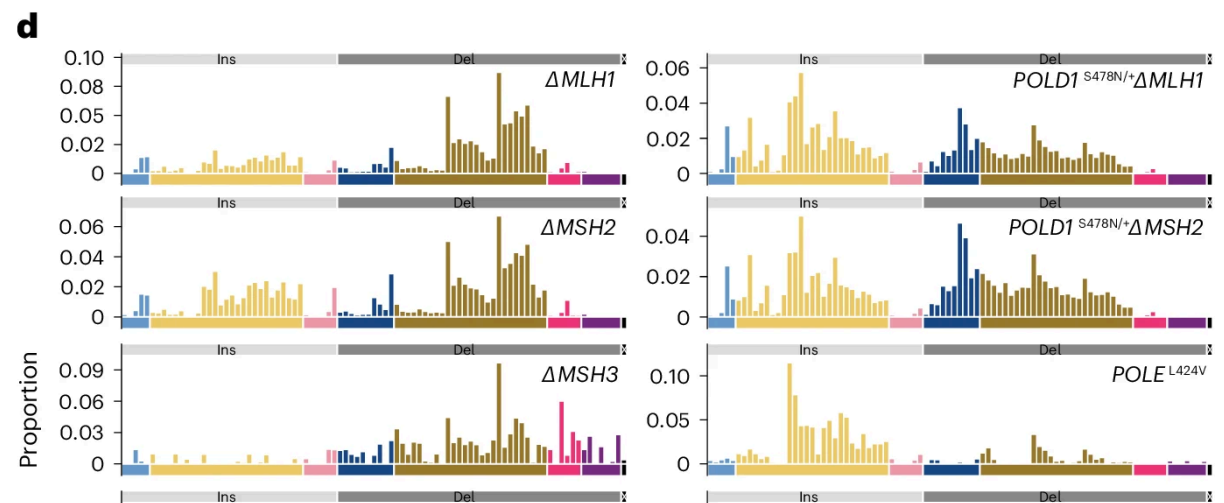
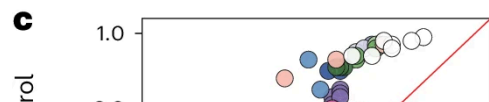
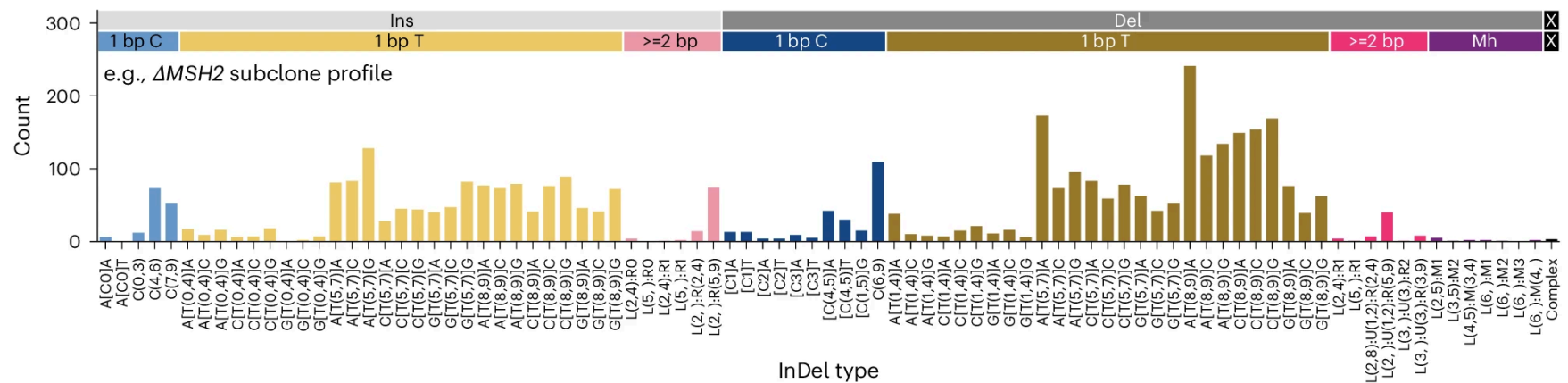
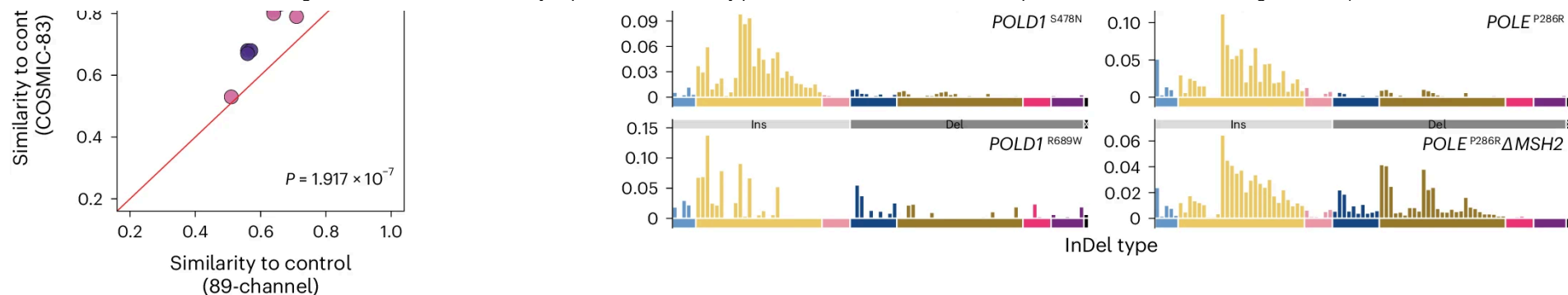


[nature](#) > [nature genetics](#) > [articles](#) > [article](#) > figure

Fig. 2: Redefined InDel taxonomy improves discriminatory power and reveals differential InDel patterns associated with PRR gene edits.

From: [A redefined InDel taxonomy provides insights into mutational signatures](#)





a, Proposed InDel classification schema and an example 89-channel InDel profile of an Δ MSH2 subclone. **b**, Distinguishing 89-channel InDel profiles of edited subclones from background control. Light blue error bars depict the mean \pm 3 s.d. of cosine similarities between $n = 100$ bootstrapped InDel profiles of unedited controls and the background profile (Extended Data Fig. 5b) aggregated from $n = 7$ unedited subclones. The x axis shows the InDel count in log scale. **c**, Cosine similarities of edited subclones and bootstrapped controls in COSMIC-83 InDel profiles against 89-channel InDel profiles. Two-tailed Wilcoxon signed-rank test, $P = 1.917 \times 10^{-7}$). **d**, The 89-channel InDel mutational signatures associated with PRRd gene edits following background subtraction (Supplementary Table 4; <https://signal.mutationalsignatures.com/explore/main/experimental/experiments?study=7>). Ins, insertion; Del, deletion.

[Back to article page >](#)